STM and atomic-resolution noncontact AFM of an oxygen-deficient $TiO_2(110)$ surface

M. Ashino* and T. Uchihashi
Joint Research Center for Atom Technology, 1-1-4 Higashi, Tsukuba 305-0046, Japan

K. Yokoyama
Graduate School of Engineering, Osaka University, 2-1 Yamada-oka, Suita, 565-0871, Japan

Y. Sugawara
Joint Research Center for Atom Technology, 1-1-4 Higashi, Tsukuba 305-0046, Japan
and Graduate School of Engineering, Osaka University, 2-1 Yamada-oka, Suita, 565-0871, Japan

S. Morita
Graduate School of Engineering, Osaka University, 2-1 Yamada-oka, Suita, 565-0871, Japan

M. Ishikawa
Joint Research Center for Atom Technology, 1-1-4 Higashi, Tsukuba 305-0046, Japan
(Received 20 January 2000)

We present atom-resolved images of oxygen-deficient $TiO_2(110)$ by scanning tunneling microscopy (STM) and noncontact atomic force microscopy (NC-AFM). Although STM images emphasized variations of Ti-atom density underneath the surface oxygen, NC-AFM images directly traced defect-induced structures of topmost oxygen atoms. We first found the (1×3) phases was not composed of missing TiO_2 units but added Ti_2O_3 rows. We observed the deformed (1×3) phase by half steps along [001], which well explains that diffusion and adsorption of segregated impurities help in the formation of (1×3) phases.

Rutile $TiO_2(110)$ surfaces have extensively been investigated as a representative system of easily-reducible *d*-type nonmagnetic metal oxides. Oxygen-deficient surface structures are regarded as a predominant factor for their chemical and electronic properties, essential to preparing high-efficient catalysts, solar cells, gas sensors, photoelectrolytes of water, and so on. Recently, a large number of studies have been devoted to understanding those structures.[1–14] Xu *et al.* reported that the primitive (1×1) phases are formed below 700 K and between 900 and 1150 K, whereas the (1×2) phases, known as partially reduced reconstruction having double periodicity along $[\bar{1}10]$, are formed between 700 and 800 K and above 1200 K.[5,8] Oxygen-deficient structures such as point defects and defect clusters in (1×1) and (1×2) phases were studied by scanning tunneling microscopy (STM) (Refs. 1–9) and noncontact atomic force microscopy (NC-AFM).[10] Moreover, the half steps caused by crystallographic shear (CS) planes, a formation of planar defect clustering in flashing or annealing at elevated temperatures ($\geqslant$970 K), were investigated by STM.[11–13]

For the (1×2) phases, two structural models, the added Ti_2O_3-row model[1] and the missing TiO_2-unit model,[6] are widely accepted by a variety of experimental observations and theoretical calculations. Recently, Bennett *et al.* proposed the coexistence of two such structures in (1×2) phases from their reoxidation experiments.[9] In contrast to a large number of studies for the (1×1) and (1×2) phases, there are only a few reports for other phases. Berkó and Solymosi found that (1×3) phases as one of $(1\times n)$ series reconstructions appeared during transition from (1×1) to (1×2) phases.[4] They observed two kinds of structures having three times the periodicity along $[\bar{1}10]$: one has wide strings and the other has narrow strings. Pang *et al.* observed (1×3) phases exhibiting the missing TiO_2-unit structures,[6] which are equivalent to the wide strings in Ref. 4. Nörenberg *et al.* observed (1×3) phases on an oxygen-deficient surface including half steps along $[\bar{1}10]$, $[\bar{1}\bar{1}1]$, and $[\bar{1}11]$.[12] They proposed a possible mechanism of the (1×3) phase formation involving calcium segregation induced by CS formation. However, they did not perform atomic-scale observations to explain the mechanism of the (1×3) reconstruction owing to segregated calcium.

In this paper we present atom-resolved STM and NC-AFM images of an oxygen-deficient $TiO_2(110)$ surface. We found the (1×3) phases not composed of missing TiO_2 units but added Ti_2O_3 rows, which are equivalent to the narrow strings in Ref. 4. We observed the (1×3) phase deformed by half steps along [001]. On the basis of the idea that the half step formation has close relations with both CS formation and diffusion of segregated impurities, we propose that (1×3) phases terminated with added Ti_2O_3 rows are formed by diffusion and adsorption of segregated impurities, together with diffusion and adsorption of Ti_2O_3 on the surface along the [001] direction. The key technology to observe the half steps is the use of NC-AFM. STM usually visualizes Ti atoms underneath the surface oxygen layer[8] and emphasizes the variation of Ti-atom density in defect-induced structures. On the other hand, NC-AFM visualized bridging-oxygen atoms in (1×1) phases[10] and in the present study directly visualized the surface oxygen atoms forming the half steps and the added Ti_2O_3 rows. It is widely ac-

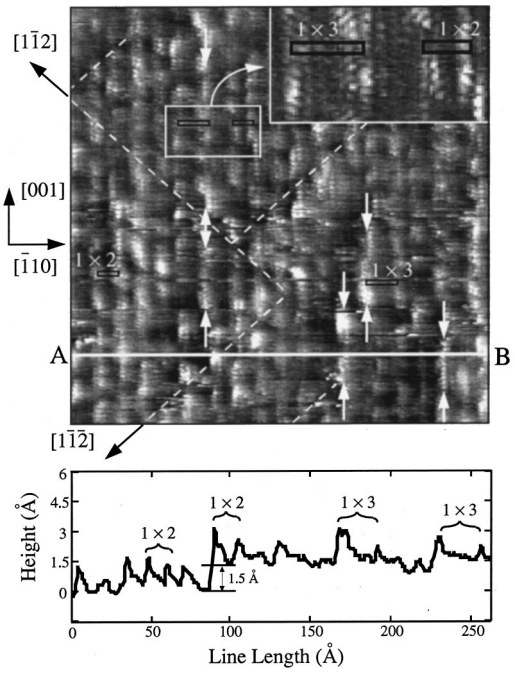

FIG. 1. STM image of $TiO_2(110)$(260×260 Å^2, $V_s=+2.3$ V, $I_t=0.4$ nA). The cross section of A-B is shown in the lower recording. Broken lines indicate half steps along $[1\bar{1}2]$ and $[1\bar{1}\bar{2}]$. (1×3) phases in addition to (1×2) phases are shown with unit cells. The area enclosed by an open rectangle is magnified in the inset to confirm (1×2) and (1×3) phases. Brighter rows higher than 2.0 Å are denoted by pairs of arrows.

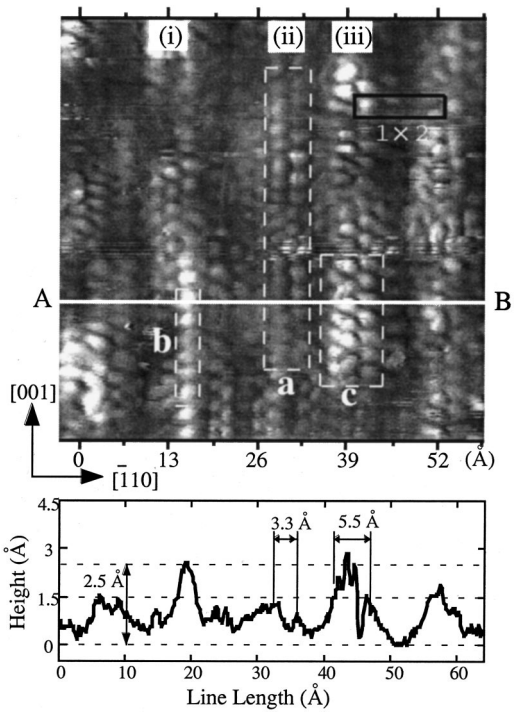

FIG. 2. Atom-resolved STM image (62×62 Å^2, $+2.3$ V,0.8 nA), and the cross section of A-B (lower record). The enclosed areas labeled ''a'', ''b'', and ''c'' were composed of two rows ($\sim$1.5 Å height), one row ($\sim$2.5 Å height), and three rows ($\sim$2.5 Å height) of atomic features, respectively. The distance between (i)-(ii) and (ii)-(iii) rows differs from the horizontal length of a unit cell of (1×2). The distances between atomic features are presented in the lower record.

cepted that NC-AFM does not always trace accurately the surface topography[14,15], while in our study NC-AFM images of a $TiO_2(110)$ surface produced surface topography.

The experiments were performed under ultrahigh vacuum (UHV) conditions using a home-built scanning probe microscope, which can operate as an STM and NC-AFM. The base pressure was in the 10^{-11}-Torr regime. A commercial PtIr-tip (Nanotips) cleaned by Ar^+ bombardments was used in the STM observation. In the NC-AFM measurement, a commercial n^+-silicon cantilever (NANOSENSORS) with a spring constant $k=41$ N/m and a mechanical resonant frequency $f_0=171$ kHz was used as a force sensor after cleaning by Ar^+ bombardment. To sense tip-sample interaction in the attractive force regime with high sensitivity, a frequency modulation technique was used under resonant oscillation conditions of the cantilevers with high-Q values ($>30\,000$) in UHV.[15] The amplitude of the excitation voltage applied to a piezoactuator was kept constant through the whole measurement. The oscillation amplitude of the cantilever was $\sim$87 Å. A polished $TiO_2(110)$ substrate of $2\times10\times0.3$ mm^3 (Earth Chemicals Co., Japan) was cleaned by repeated cycles of Ar^+ bombardment ($\sim$3 keV,200 nA) and annealing at increasing temperature finally to $\sim$1250 K for every 5–15 min in UHV ($<3\times10^{-10}$ Torr), and turned into a deep-blue crystal.

Figure 1 shows a constant current topographic STM image of empty states of $TiO_2(110)$ and the cross section of a line A-B. The presented area, where bright rows with 1.5 ±0.1 Å corrugations were running along the [001] direction, was part of a terrace spread over 400 Å wide between single steps (3.2 ± 0.1 Å height). From the distances between these bright rows, we found that the surface was composed of (1×2) and (1×3) phases. Moreover, Fig. 1 shows that the surface included half steps along $[1\bar{1}2]$ and $[1\bar{1}\bar{2}]$, which are equivalent to those caused by the CS planes belonging to the {132} family for $TiO_{1.90}-TiO_{1.9375}$.[13] Also, along [001] the brighter rows of higher than 2.0 Å were included in (1×3) phases, as denoted by pairs of arrows.

Figure 2 shows an atom-resolved STM image and the cross section of a line A-B, which were obtained at an area neighboring on the left side of Fig. 1 (not shown in Fig. 1). An apparent height of [001] rows was not uniform and classified into two kinds, namely, $\sim$1.5 Å and $\sim$2.5 Å (see the cross section). The rows of $\sim$1.5 Å height were mainly composed of two bright rows of atomic features (see the enclosed area labeled ''a'') with almost the same periodicity along [001] as a unit cell ($a_{001}=3.0$ Å). In the area a the distance between such atomic features was 3.3 ± 0.2 Å in the $[\bar{1}10]$ direction, which is consistent with the distance between Ti atoms in the added Ti_2O_3 rows.[1] On the other hand, the rows of $\sim$2.5 Å height were composed of single or triple rows of atomic features, each of which corresponds to the area labeled ''b'' or ''c'', respectively. The distance between outside rows of triple features was 5.5 ± 0.2 Å, which is close to the dimension of the missing TiO_2-unit structure.[6] Thus, the STM image obtained appears to be composed of both structures of added row and missing unit, as reported in Ref. 9.

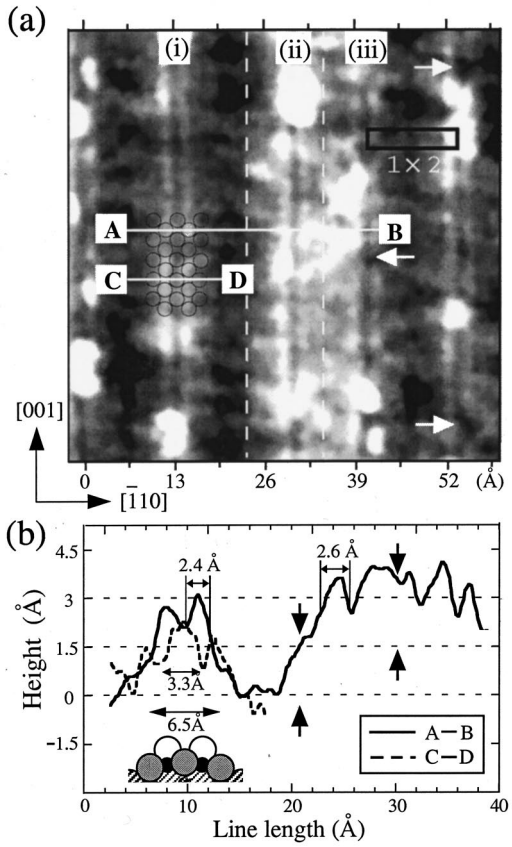

FIG. 3. (a) An atom-resolved NC-AFM image of the same row arrangement as Fig. 2 shows (62×62 Å^2), including single oxygen vacancies at the positions denoted by open arrows and segregated impurities at the sites with extra brightness. The controlled frequency shift was $\Delta f\sim-14.7$ Hz. A bias voltage (-0.7 V) was applied for obtaining high contrast. A ball model of the added Ti_2O_3 row and a unit cell of (1×2) are put on the corresponding positions. (b) Cross sections of two line segments *A*-*B* and *C*-*D* in (a) and a ball model of the added Ti_2O_3 row. Large circles (open and shaded) and small filled circles represent oxygen atoms and Ti atoms, respectively. The width of protrusions and the distances between Ti atoms and bridging oxygen are also shown. Pairs of arrows indicate the position of half steps.

Figure 2 also indicates that the distance between the [001] row labeled (i) and the row labeled (ii) is larger than $2a_{\bar{1}10}=13$ Å and that the distance between the (ii) row and the (iii) row is smaller than $2a_{\bar{1}10}=13$ Å. However, from the image presented in Fig. 2 it is difficult to explain how such irregularity was induced, and moreover, how such irregularity was related to two or three kinds of structures that appeared at the areas *a*, *b*, and *c*. STM mainly visualized the empty states of Ti atoms underlying topmost oxygen atoms on TiO_2 surfaces. Figure 2 does not directly represent the oxygen-deficient structures but the variations of Ti-atom density. On the other hand, the NC-AFM image represents surface structures of topmost oxygen atoms, as pointed out in the previous study of $TiO_2(110)$-(1×1),[10] and makes it possible to directly represent oxygen-deficient structures of TiO_2 surfaces.

Figure 3(a) shows a NC-AFM image obtained from almost the same area, having the same arrangement of [001] rows, as the STM image (Fig. 2) was obtained. In Fig. 3(a) each row along the [001] direction was composed of centered two bright rows and outside two faint rows of atomic features. The separation of these atomic features along the [001] direction was approximately consistent with $a_{001}=3.0$ Å. The distance in the $[\bar{1}10]$ direction was 3.2 ± 0.2 Å between the bright rows and 6.8 ± 0.3 Å between the faint rows. The cross sections through the line segments *A*-*B* and *C*-*D* are plotted with a solid line and a dotted line in Fig. 3(b), respectively. Comparing the left records of Fig. 3(b), corresponding to the row labeled (i) in Fig. 3(a), with the cross-sectional ball model of the added Ti_2O_3-row structure drawn below in the same dimension, we found that the dotted line traces the outline of the shaded circles, while the solid line traces the outline of the open circles. In the cross-sectional ball model the shaded circles represent the bridging two oxygen atoms and a bottom oxygen atom of Ti_2O_3; the open circles represent topmost two oxygen atoms of Ti_2O_3. Thus, each row along the [001] direction in Fig. 3(a) directly corresponds to added Ti_2O_3 and two bridging oxygen atoms.

In Fig. 3(b) the width of the protrusions was 2.4-2.9 Å, which is close to twice the van der Waals radius of oxygen (1.40 Å). Moreover, the corrugation of *A*-*B* line is approximately 3 Å on the left record corresponding to the (i) row in Fig. 3(a), which is equivalent to the known single step height (3.25 Å),[1] namely, the height from in-plane oxygen to topmost oxygen. Therefore, we concluded that the surface oxygen atoms were preferentially visualized in the NC-AFM image and that Fig. 3 demonstrates that NC-AFM images directly trace the true surface topography of $TiO_2(110)$ in contrast to other semiconductor surfaces.[14,15] From this point of view, we found the formation of two half steps at the positions denoted by pairs of arrows on the right record in Fig. 3(b). These positions correspond to the broken lines along the [001] direction in Fig. 3(a). The irregularity of the rows in Fig. 3(a) [also in Fig. 2(a)] is expected to have a close relation to such half steps.

Figure 4(a) represents a structural model without geometric imperfections, while Fig. 4(b) represents a structural model of the irregularity of the rows, put on the corresponding positions of the lower part of Fig. 3(a). In Fig. 4(b) the atomic arrangement of the row labeled (ii) is out of phase with the other rows by half a unit cell along the [001] direction as shown in the crosses marked on topmost oxygen atoms. The displacement in the $[\bar{1}10]$ direction is caused by the deficiency of two rows of in-plane oxygen corresponding to the two rows enclosed by red open rectangles in Fig. 4(a). Because the prepared surface included the half steps along $[1\bar{1}2]$ and $[1\bar{1}\bar{2}]$ caused by the CS planes belonging to the {132} family (Fig. 1), the similar CS process is considered to reproduce the half steps between the (i)-(ii) rows and the (ii)-(iii) rows. The CS displacement is denoted as $\frac{1}{2}[0\bar{1}1]$ with a lattice vector,[13] which is equivalent to the CS operation $\frac{1}{2}[011]=\frac{1}{4}[110]+\frac{1}{2}[001]+\frac{1}{4}[\bar{1}10]$, in Ref. 12. Thus, the displacement in the [110] direction is estimated at ~1.6 Å ($\frac{1}{4}a_{110}$), to which the evaluated value ~1.5 Å in Fig. 3(b) is close. In Fig. 3(a) the half steps corresponding to this displacement ran along the [001] direction. These, to our knowledge, have not been previously reported but are findings observed in this work. It is possible for the $(\bar{1}10)$ plane,

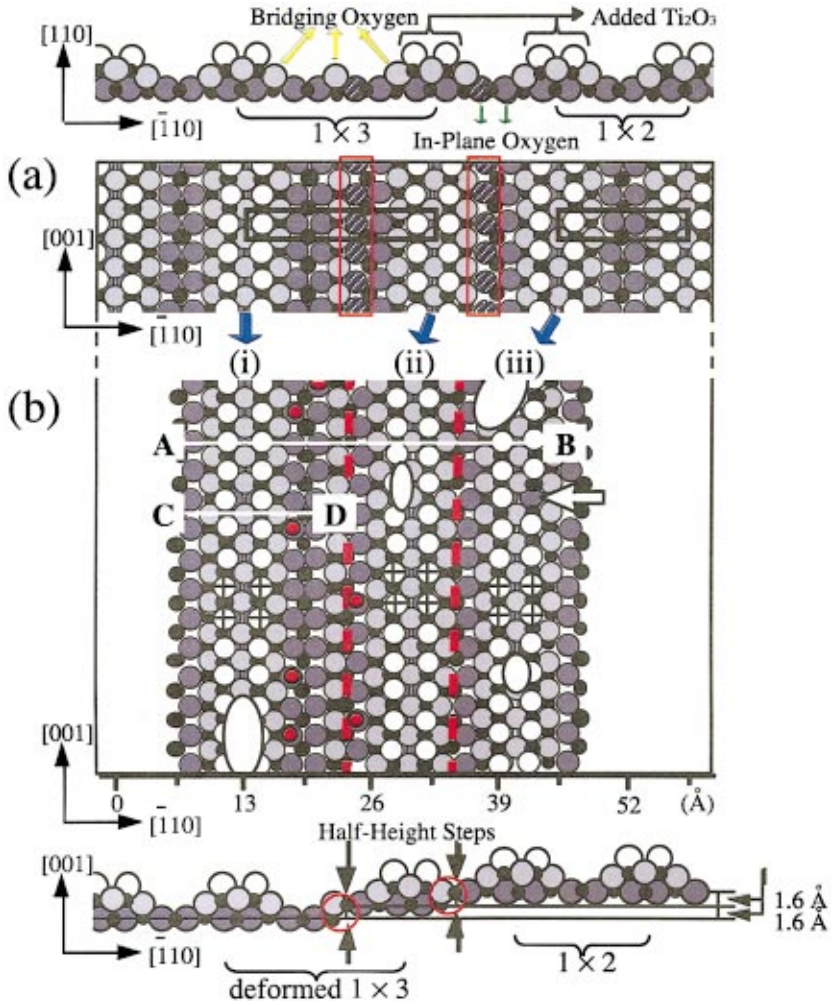

FIG. 4. (Color) Structural models representing formation of half steps along [001]. (a) A structural model before the formation of half steps. Unit cells of (1×3) and (1×2) are outlined by black open rectangles. Segregated impurities are considered to be adsorbed on the slash-marked positions. (b) A schematic reproduction of row arrangement, put on the corresponding positions of the lower part of Fig. 3(a). Open ellipses lie on the same sites with extra brightness as Fig. 3(a) shows. The line segments *A*-*B* and *C*-*D* and the arrows (white) lie on the same positions. Crosses mark topmost oxygen atoms to clearly indicate the displacement of the (ii) row along [001]. Red closed circles represent the adsorption of the segregated impurities on the in-plane oxygen atoms between the rows (i)-(ii). Cross sectional drawings of (a) and (b) are also shown in the top and the bottom, respectively. Comparing (b) with (a), the distance between the rows labeled (i) and (ii) and the distance between the rows labeled (ii) and (iii) are shortened by lacking each of the in-plane oxygen rows enclosed by red open rectangles in (a). The half steps are running on the positions of red broken lines. Overlapping of Ti atoms is indicated by open red circles in the cross sectional drawings of (b). In these atomic models we used the same notations as in Fig. 3.

which is one of the thermodynamically most stable faces, to move along [001] and [$\bar{1}$10] directions, together with the CS plane formation, and consequently to form the half steps along the [001] direction.

Comparing Fig. 2 with Figs. 3 and 4, we conclude that the STM images does not always present the half steps along the [001] direction. Although the STM image (Fig. 2) appears to be composed of both the added Ti_2O_3-row and the missing TiO_2-unit structures, the NC-AFM image (Fig. 3) reveals that the surface did not contain the missing TiO_2-unit structures but contained only the added Ti_2O_3-row structures. As shown in the cross-sectional drawing of Fig. 4(b), the overlapping of Ti atoms at the position of the half steps can make the apparent height increase in the STM image. The NC-AFM image (Fig. 3) presents single atom vacancies in the added rows, not visualized yet in the STM images,[1] as the dark spots denoted by arrows. Also, the adsorbed impurities were visualized as clusters with extra brightness on and/or across the centered two bright rows. The added Ti_2O_3 row is inactive to anions, e.g., formate ions.[1] The clusters with extra brightness can be regarded as segregated impurities of metallic species such as calcium,[12] which strongly bonds to oxygen. Thus, the atomic features of $\sim$2.5 Å height in Fig. 2 may be the atomic arrangement of segregated impurities.

Although the segregated impurities were not identified in our study, calcium is generally accepted as one of the most popular species of segregated impurities. The (1×3) configuration is involved in calcium segregation inducing CS formation.[12] Segregated Ca atoms are adsorbed on the in-plane oxygen atoms like in a perovskite $CaTiO_3$ structure.[16] The channels formed by the octahedra allow anisotropic diffusion of metal cations along [001].[1,17] Also, Ca-O diffusion to the surface may be an important process in the creation of oxygen vacancies.[12] On the basis of these ideas we propose

mechanisms for two kinds of reconstructions, namely, the (1×3) reconstruction and the deformed (1×3) reconstruction identified in our current work. The first one is formed by the following steps: Segregated impurities observed as clusters with extra brightness in Fig. 3(a), together with a unit of Ti_2O_3, diffuse and are adsorbed on in-plane oxygen of a (1×1) substrate. Adsorption of segregated impurities on one row of in-plane oxygen prevents the (1×1) configuration taking a (1×2) configuration, and consequently forces it into a (1×3) configuration. In fact, Fig. 3(a) presents some bright protrusions indicating adsorption of the segregated impurities on the in-plane oxygen atom sites. The corresponding positions between the rows (i)-(ii) are marked by red closed circles in Fig. 4(b). The second deformed reconstruction is formed by the following steps: After segregated impurities bond to in-plane oxygen atoms, the segregated impurities bound to oxygen diffuse on the surface leaving a row of in-plane oxygen vacancies behind themselves. The oxygen vacancy consequently deforms the (1×3) reconstruction, together with the formation of half steps along [001]. Figure 4 shows that the deficiency of one row of in-plane oxygen caused the half step between the (i)-(ii) rows, followed by the deformation of the (1×3) configuration.

In summary, we observed the rows of atomic features along [001] in (1×2) and (1×3) phases of oxygen-deficient $TiO_2(110)$ by STM and NC-AFM. We found the (1×3) phases composed of added Ti_2O_3 rows, corresponding to the narrow strings reported by Berkó and Solymosi. Although STM emphasized the variation of Ti-atom density, NC-AFM provided surface topography and demonstrated the half steps along [001], which holds the key to understanding the (1×3) reconstruction.

The authors thank H. Onishi, C.L. Pang, P. Käckell, and T. Uda for fruitful discussions.

*Author to whom correspondence should be addressed. Electronic address: ashino@jrcat.or.jp

[1] H. Onishi and Y. Iwasawa, Surf. Sci. **313**, L783 (1994); H. Onishi, K. Fukui, and Y. Iwasawa, Bull. Chem. Soc. Jpn. **68**, 2447 (1995).
[2] A. Szabo and T. Engel, Surf. Sci. **329**, 241 (1995).
[3] S. Fischer *et al.*, Surf. Sci. **337**, 17 (1995).
[4] A. Berkó and F. Solymosi, Langmuir **12**, 1257 (1996).
[5] C. Xu *et al.*, Phys. Rev. B **56**, 13 464 (1997).
[6] C.L. Pang *et al.*, Phys. Rev. B **58**, 1586 (1998).
[7] U. Diebold *et al.*, Surf. Sci. **411**, 137 (1998).
[8] R.E. Tanner, M.R. Castell, and G.A.D. Briggs, Surf. Sci. **412/413**, 672 (1998).
[9] R.A. Bennett *et al.*, Phys. Rev. Lett. **82**, 3831 (1999).
[10] K.I. Fukui, H. Onishi, and Y. Iwasawa, Phys. Rev. Lett. **79**, 4202 (1997).
[11] G.S. Rohrer, V.E. Henrich, and D.A. Bonnell, Science **250**, 1239 (1990); Surf. Sci. **278**, 146 (1992).
[12] H. Nörenberg *et al.*, Surf. Sci. **396**, 52 (1998).
[13] R.A. Bennett *et al.*, Phys. Rev. B **59**, 10 341 (1999).
[14] F.J. Giessibl, Science **267**, 68 (1995); S. Kitamura and M. Iwatsuki, Jpn. J. Appl. Phys., Part 2 **34**, L145 (1995); P. Guthner, J. Vac. Sci. Technol. B **14**, 2428 (1996).
[15] Y. Sugawara *et al.*, Science **270**, 1646 (1995).
[16] L.P. Zhang, M. Li, and U. Diebold, Surf. Sci. **412/413**, 242 (1998).
[17] J.L. Steele and E.R. McCartney, Nature (London) **222**, 79 (1969).